HAL open science

Experimental Identification of Fluid Thin Film Dynamic Coefficients for Space Propulsion Turbo Pumps

Pascal Jolly, Olivier Bonneau, Mihai Arghir, Romain Gauthier, Jérôme Dehouve

To cite this version:

Pascal Jolly, Olivier Bonneau, Mihai Arghir, Romain Gauthier, Jérôme Dehouve. Experimental Identification of Fluid Thin Film Dynamic Coefficients for Space Propulsion Turbo Pumps. 17th International Symposium on Transport Phenomena and Dynamics of Rotating Machinery (ISROMAC2017), Dec 2017, Maui, United States. hal-03004970

HAL Id: hal-03004970

https://hal.science/hal-03004970v1

Submitted on 13 Nov 2020

HAL is a multi-disciplinary open access archive for the deposit and dissemination of scientific research documents, whether they are published or not. The documents may come from teaching and research institutions in France or abroad, or from public or private research centers.

L'archive ouverte pluridisciplinaire **HAL**, est destinée au dépôt et à la diffusion de documents scientifiques de niveau recherche, publiés ou non, émanant des établissements d'enseignement et de recherche français ou étrangers, des laboratoires publics ou privés.

Distributed under a Creative Commons Attribution 4.0 International License

Experimental Identification of Fluid Thin Film Dynamic Coefficients for Space Propulsion Turbo Pumps

Pascal Jolly[1]*, Olivier Bonneau[1], Mihaï Arghir[1], Romain Gauthier[2], Jérôme Dehouve[3]

ISROMAC 2017

International Symposium on Transport Phenomena and Dynamics of Rotating Machinery

Maui, Hawaii

December 16-21, 2017

Abstract

Through an application example, a test rig dedicated to the measurement of rotordynamic coefficients for thin fluid film components, as encountered in liquid Rocket Engine Turbopump, is presented. Low viscosity fluids (as cryogenic fluids), leads to thin film flows with high Reynolds number. Tests are performed with a Reynolds similitude, using warm water and a component's nominal diameter about ten times larger than the prototype (for bearings and seals). Typical results are presented for a front shrouded centrifugal pump impeller, using various kinds of eye-packing seals and a vaned diffuser. All the tests have been operated with a centered position of the rotor. For various rotor speeds, experimental data (displacements, forces, pressures, flowrate, temperatures, torque) have been recorded for steady-state static case and dynamic excitations (frequency range from 20 to 80 Hz in 10 Hz increments). First, the performance curves are discussed. Then, the identified dynamic coefficients are presented.[?]

Keywords

Test Rig — Dynamic Coefficients — Turbopump — Impeller

[1] *Institut Pprime CNRS, Université de Poitiers, ISAE ENSMA, Poitiers, France*

[2] *ARIANE GROUP, Vernon, France*

[3] *CNES DLA, Evry, France*

*__Corresponding author__: pascal.jolly@univ-poitiers.fr

INTRODUCTION

In order to estimate vibration levels caused by fluid-structural interactions, designers of turbopumps can use rotordynamic models, where input parameters for each component acting on the rotor (bearings, seals, impellers) consist in linearized dynamic coefficients. In the case of thin fluid film components (like labyrinth seals and fluid bearings), fluid inertia effect is significant and it is good to validate theoretical simulations against experimental results. A consortium of French companies (CNES, ASL, EDF R&D, ALSTOM) together with CNRS (French Scientific Research Center) and the University of Poitiers have built a test rig specially dedicated to the experimental analysis of these fluid components. This test rig named BALAFRE ("BAnc LAmes Fluides à haut nombre de REynolds") measures the displacements induced by dynamic excitations and the resulting fluid film responses. These measurements enable the identification of the dynamic behavior (stiffness, damping and added mass) of fluid bearings, seals or impellers. The paper describes the test rig and some typical results obtained for a centrifugal impeller.

1. TEST FACILITY

The test rig BALAFRE (BAnc LAmes Fluides à haut nombre de REynolds) is dedicated to the identification of dynamic force coefficients of thin fluid film components of high speed rotating machines. These components often use a low viscosity process fluid as lubricant (in cryogenic applications for example). Therefore, the flow in the thin fluid film exhibits high Reynolds numbers. In order to reproduce experimentally these high Reynolds numbers regimes, the test rig uses hot water as lubricant (temperatures limited to 50°C), inlet pressure as high as 45 bar and tested components can have a nominal diameters up to 350 mm. These conditions lead to axial and circumferential Reynolds number up to 10^5. The test rig is mainly composed of a test cell, an electric motor, a hydraulic system (with pumps, tanks, filters and valves) and a Programmable Logic Controller associated with DAQ device. A cross section view of the test cell is shown in Figure 1, where the tested component (an annular seal in the present configuration) is overhung mounted at the left end of a rotating shaft $\boxed{7}$. The rotor and the stator of the annular seal are respectivelly indicated as $\boxed{1}$ and $\boxed{2}$. This design gives a great modularity to the test cell, where various kinds of components have benn mounted : seals, hydrostatic bearings and impellers.

The whole test rig is pressurized at 5 bar. This means that an annular seal can have a maximum pressure difference of 40 bar between the upstream and the downstream (discharge) chambers. The necessary flow rate (up to 120 m^3/h) is delivered by two centrifugal pumps driven by electrical motors whose total power is 330 kW. The maximum shaft speed (6000 rpm) is obtained with a three-phase asynchronous motor of 180 kW. A double conical hydrostatic thrust bearing is lo-

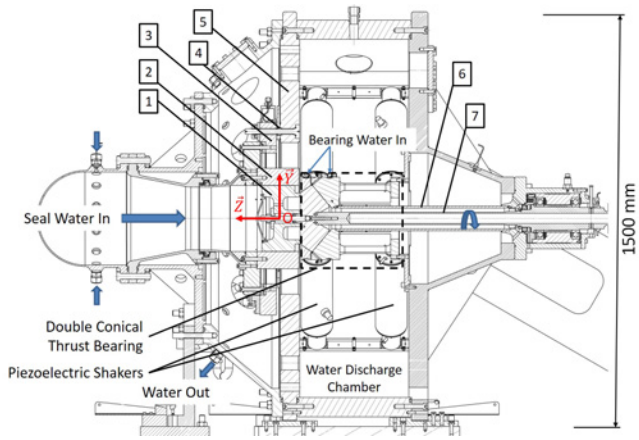

Figure 1. Cross sectional view of the test rig

cated close to the test component. It has many roles: first it must guide the rotation of the shaft and support the static axial load (which can reach as much as 200 kN) generated by the 40 bar pressure difference between the two faces of the annular seal. Its second role is to transmit the excitations imposed by the 8 piezoelectric actuators mounted four by four along two planes. The housing of the bearing is linked to the frame via a hollow tube $\boxed{6}$ designed to be very stiff axially and flexible in the radial direction. The first natural frequency of the bending mode of the shaft is 460 Hz; the two first natural frequencies of the torsional modes are 14 Hz and 269 Hz. The double conical hydrostatic thrust bearing is provided with $2x6$ recesses and orifice restrictors [1] and is fed with water at 150 bar. The average fluid film thickness in the two parts of the bearing is about 40 μm and the axial and radial stiffnesses are larger than $10^9\ N/m$.[1]. The outlet flow from both the tested component and the double conical hydrostatic thrust bearing is discharged in the test rig and then returns to a water tank of $5\,m^3$ via several hoses and pipes. Dynamic displacements are applied to the rotor by 8 piezoelectric shakers, mounted 4 by 4 in the forward and in the rear plane of the double conical hybrid bearing. The maximum dynamic displacements are $\pm 100\ \mu m$ with a frequency range from 20 to 200 Hz, corresponding to dynamic loads of 20 kN per axis[2]. The housing $\boxed{2}$ of the tested component is fixed on a rigid part $\boxed{3}$ which is mounted on the test rig's frame $\boxed{5}$ via three piezoelectric force transducers (Kistler 9167) $\boxed{4}$ each one being able to measure three components, in a range $[-20\ kN; 20\ kN]$. Their stiffnesses are respectively $4.6x10^9\ N/m$ and $1.67x10^9\ N/m$ in directions Z and X,Y. For each axis, the proportional error is $\leq \pm 1\,\%$ and the hysteresis is $\leq 2\,\%$, both for the full scale output. The three sensors constitute a force balance. The first natural frequency of the axial mode of the stator assembly (housing and force sensors) is 280 Hz. The two first natural frequencies of the bending mode are 370 Hz and 520 Hz. The housing is equipped with 6 eddy current proximity probes (Bently Nevada 3300 XL 8mm), positioned three by three in the front and rear plane (for an annular seal or a hydrostatic bearing). Their linearity error is $\leq 5\,\%$. These sensors measure the relative displacements between the rotor and the housing. Therefore, the position of the rotor center in the two planes as well as the radial clearance can be deduced. Before each test, a dedicated part, having an outside diameter that fits exactly the housing's inside diameter, is used to calibrate simultaneously the response (gain and offset) of the 6 displacement sensors. Misalignment of the rotor can also be obtained knowing that the two measuring planes are equidistant from the housing midplane. Three accelerometers are also mounted on the housing enabling the measurement of its absolute movements.

[1]The stiffnesses of the double conical hydrostatic thrust bearing are high contrary to those of the tested component in order to lower the power of the shakers

[2]The power of the shakers is set to a percentage of their total power. Therefore, the obtained amplitudes of displacements of the rotor depend on the direct stiffnesses of the tested component

2. DYNAMIC COEFFICIENTS IDENTIFICATION

In many works, known orbiting motions are imposed to the impeller (whirling motion is produced by an eccentric drive mechanism) and resulting hydrodynamic forces are measured [2, 3, 4]. According to a mass-damping-stiffness model, implying that the hydrodynamic force matrix $|A|$ is quadratic with in ω/Ω (whirl motion speed to shaft speed ratio), rotordynamic coefficients matrices are then obtained from a least squares fit. In [5], measurements are performed using a hydraulic exciter to impose transient excitations (up to 50 Hz) to the impeller in one direction of motion (vertical translation). In [6], an experimental apparatus equipped with active magnetic bearings is used to measure fluid film forces while imposing a whirling orbit to impellers.

Here, the dynamic displacements of the rotor imposed by the shakers generate fluid forces that the housing transmits to the piezoelectric force transducers (acting like high stiffness springs). For lateral displacements of the rotor along $vecx$ and $vecy$ axes of the coordinate system defined in Figure 1, the equations of the fundamental principle of dynamics applied to the housing with respect to the center of the component O are:

$$\begin{cases} m\ddot{x} = -f_x + \sum_{k=1}^{3} fb_x^k \\ m\ddot{y} = -f_y + \sum_{k=1}^{3} fb_y^k \end{cases} \tag{1}$$

where f and fb^k are respectively the fluid film forces and the forces measured by the kth sensor of the force balance while the subscript x and y denote their directions. For an excitation frequency in the range 20 to 120 Hz, the accelerations of the housing can be neglected [7], and eq. 1 can be

simplified as:

$$\begin{cases} f_x = \sum_{k=1}^{3} f b_x^k \\ f_y = \sum_{k=1}^{3} f b_y^k \end{cases} \tag{2}$$

Introducing the small perturbation hypothesis, fluid film forces can be described by linear dynamic coefficients (stiffness K, damping C and added mass M) or impedances Z. In the frequency domain (after applying the Fourier transform), the fluid film forces and the displacements of the rotor are written as follows:

$$\begin{cases} F_x = Z_{xx}X + Z_{xy}Y \\ F_y = Z_{yx}X + Z_{yy}Y \end{cases} \tag{3}$$

The unknown impedances Z_{xx}, Z_{xy}, Z_{yx} and Z_{yy} are found by using two linearly independent excitations (denoted by the superscripts 1 and 2) consisting in lateral vibrations obtained by successively exciting the piezoelectric shakers in two orthogonal directions and with the same phase for the front and rear planes. The impedances are computed by inverting the displacement matrix as follows:

$$\begin{bmatrix} Z_{xx} & Z_{xy} \\ Z_{yx} & Z_{yy} \end{bmatrix} = \begin{bmatrix} F_x^1 & F_x^2 \\ F_y^1 & F_y^2 \end{bmatrix} \begin{bmatrix} X^1 & X^2 \\ Y^1 & Y^2 \end{bmatrix}^{-1} \tag{4}$$

The stiffness, damping and added mass matrices of coefficients are calculated from the real and imaginary part of the corresponding impedances as follows:

$$\begin{cases} K_{ij} - M_{ij}\omega^2 = \Re\left[Z_{ij}(\omega)\right] \\ j\omega C_{ij} = \Im\left[Z_{ij}(\omega)\right] \end{cases} \tag{5}$$

with $[ij] = [xx; xy; yx; yy]$. Equation 5 shows that in order to enable the identification of constant dynamic coefficients, the real part of the impedance must describe a parabola and its imaginary part must describe a straight line. In order to perform a curve fitting by the least square procedure, the impedances are calculated for a significant number of excitation frequencies ω. An example of the real and the imaginary parts of the impedance used during the identification[3] is shown in Figure 2.

The uncertainty in K_{ij} and C_{ij} is respectively estimated to ±15 % and ±30 %.

3. TESTED IMPELLERS

Two types of centrifugal impellers were tested: open (unshrouded) and closed (front shrouded). Although the test impeller was designed to work with a cryogenic fluid, water was used as working fluid. Figure 3 gives a schematic view of the test cell with an open type impeller. Both tests were conducted with a vaned diffuser. The flowrate of water passing through the diffuser is measured by a Venturi flow rate meter located at the outlet of the volute. The leakage between the back shroud and the casing is therefore estimated since the inlet flowrate is also measured. For the open type impeller, 7 configurations were tested, consisting in changing the pressure loss downstream of the volute casing. For the closed type impeller, 6 configurations were tested, as listed in Table 1, defined by a combination of 3 types of eye-packing seal with 2 types of front casing (smooth and textured). In the present case, the 6 eddy current proximity probes are positioned by three, respectively to measure radial and axial displacements of the impeller relatively to the casing. The tests were performed by imposing only two translation degrees of freedom, from a centered position and without misalignment.

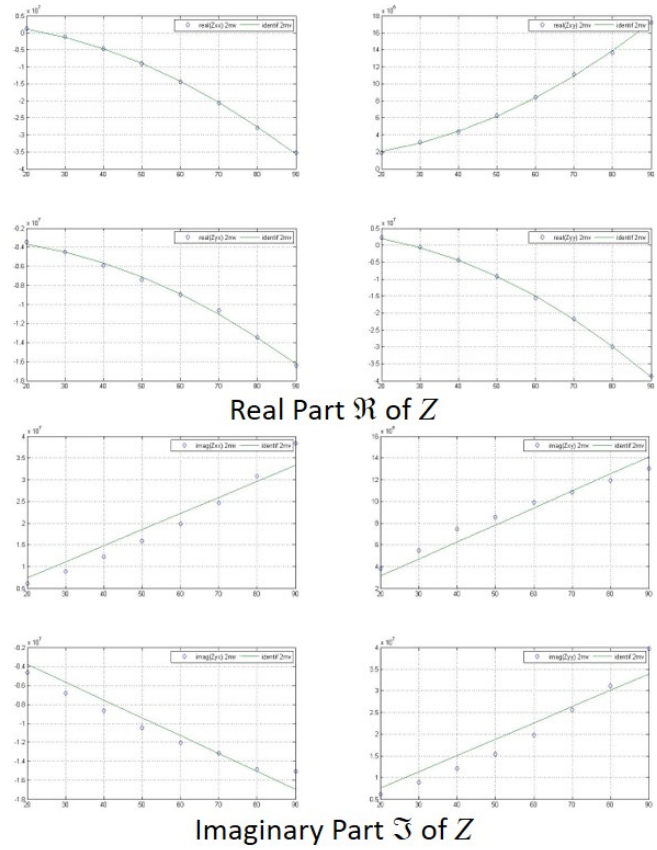

Figure 2. Curve fitting of impedance's real and imaginary parts for identification as a function of $\omega(Hz)$ in abscissa

4. TESTS CONDITIONS

All the tests have been operated with a centered position of the rotor. For each rotor speed Ω, experimental data (displacements, forces, pressures, flowrates, temperatures, torque) are recorded for steady-state static case and dynamic excitations. The tests have been performed according to the following

[3]Example corresponds to a sealing component at $\Omega = 50$, Hz

Table 1. Tested Combinations of eye-packing seal and front casing

Configuration Name	Eye Packing Seal	Front Casing
AS-S	Annular Seal	Smooth
FS-S	Face Seal	Smooth
LS-S	Labyrinth Seal	Smooth
AS-T	Annular Seal	Textured
FS-T	Face Seal	Textured
LS-T	Labyrinth Seal	Textured

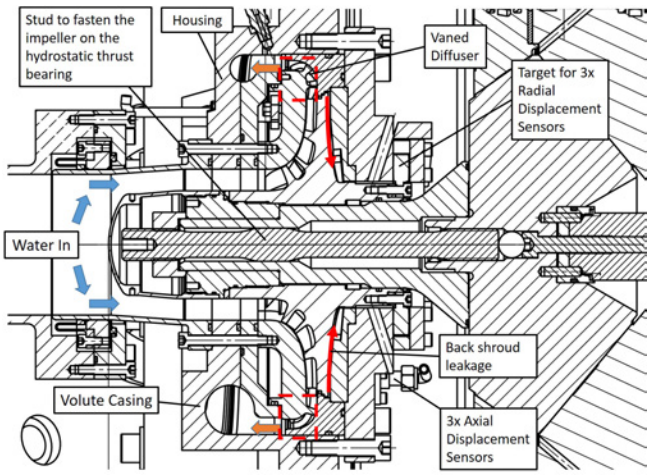

Figure 3. Cross sectional view of the test rig set up for an open type impeller

conditions :

- Rotor speed Ω: 2000, 3000, 4000 and 5000 rpm,
- Excitations frequencies ω: 20, 30, 40, 50, 60, 70, and 80 Hz,
- Water Inlet pressure P_s: 6 bar,

5. RESULTS AND DISCUSSION

In the present paper, only results corresponding to the closed type impeller are presented. Ariane Group has proceeded to many CFD simulations, using FINE™/Turbo, in order to obtain the performance curves as well as rotordynamic coefficients.

5.1 Performance curves

The open impeller has been tested first in order to find the pressure loss to install downstream of the volute casing in order to reach a given flow rate at 4000 rpm (Design Point). Then, the closed impeller has been tested with the pressure loss obtained previously. For all the tests, the flow coefficient ϕ is of the order of 0.15. Figure 4 shows the performance curves, for each combination listed in Table 1, where the pressure rise is defined as the difference between the inlet pressure of the impeller and the outlet pressure of the diffuser. Pressure and flowrate at design point are used to normalized

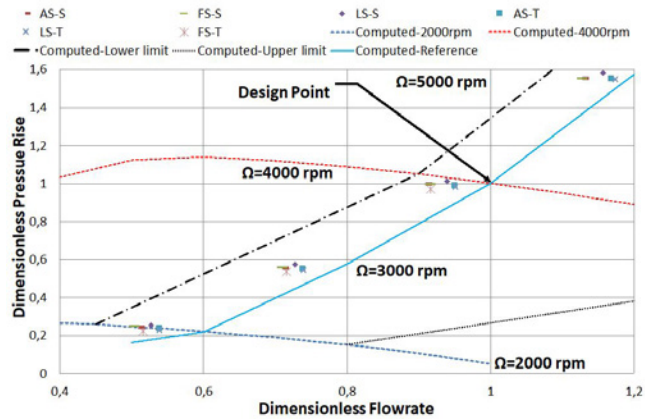

Figure 4. Performance curves in centered position

the corresponding data. The configuration $LS-T$, that corresponds to the combination of an labyrinth seal as eye-packing seal and a textured front casing, better fits the reference curve, as well as the configuration $AS-T$. Both cases show that a textured casing helps to bring points closer to the reference curve and therefore improve impeller's efficiency.

5.2 Rotordynamic Coefficients

The present experimental dynamic coefficients are made nondimensional as follows [8].

$$\begin{cases} \text{Dimensionless stiffness coefficients} \quad K^*_{ij} = \dfrac{K_{ij}}{\pi \rho r_2 b_2^2 \Omega^2} \\ \text{Dimensionless damping coefficients} \quad C^*_{ij} = \dfrac{C_{ij}}{\pi \rho r_2 b_2^2 \Omega} \end{cases} \tag{6}$$

where ρ = mass density of pumped liquid, r_2 = impeller outer (discharge) radius and b_2 = impeller discharge width including impeller side plate.

For various shaft speeds, Figures 5 show the evolution of the four term K^*_{ij} of the stiffness matrix for the 6 tested configurations. In rotordynamics, for seals and impellers, the assumption of skew-symmetric coefficient matrices (**K**, **C** and **M**) is stated to be suited [9]. However, some theoretical results in [10] are in contradiction with this. Secondly, many authors agree that, for most large impellers, the direct stiffness coefficients are negatives[4] and included in the range $[-2,5; -4,2]$ [8, 9]. As a first observation, present experimental results do not provide equal values for the direct stiffness components, at least at low rotational speed. Moreover, at $\Omega = 2000\,rpm$, K_{xx} is always negative except for the configuration $AS-T$. This configuration provides the higher levels of direct stiffnesses when the two configurations with the face seal provide very low or negative ones. A closed impeller is therefore able to provide positive direct stiffnesses

[4] As explained in [11], direct stiffness coefficients produce a radial force directed inward and collinear with the rotor deflection vector. If the coefficients are negatives, the direction of the fore reverses (outward)

beyond a rotating speed and some kinds of eye-packing seals. As a second observation, the normalized stiffnesses are of the order of one or several tens: this is higher than those above-mentioned and of the same order as in [12], obtained for an open-impeller. The normalized cross coupling stiffnesses are more in accordance with the assumption that $K_{xy} = -Kyx$ and their amplitude decrease with increasing Ω. The configurations with a textured front casing provide lower values of the cross coupled stiffness than the smooth one, showing the benefit of this design.

The normalized damping coefficients are almost constant in the range of rotating speeds. The higher direct damping is provided by the configuration $LS - T$ and the higher cross coupled damping is provided by the configuration $FS - S$. According to the above results, a closed impeller should be equipped with an annular seal and the front casing should be textured.[5]

6. CONCLUSION

A test rig dedicated to the identification of rotordynamic coefficients is presented. A set of results obtained for a closed-impeller are used to demonstrate the test rig gives, researchers and industrial supporting partners, the ability to measure stiffness and damping matrices for fluid film components as used in a liquid Rocket Engine Turbopump. In order to increase its possibilities, through a French Government program, the test rig is being modified in order to:

- perform long duration tests,
- test components fed with air.

Regarding the dynamic behavior of the present shrouded impeller, positive values of direct stiffnesses and higher levels of damping can be obtained by using a textured front casing. The annular seal is the most appropriate for this impeller while the face seal is not.

ACKNOWLEDGMENTS

The authors are grateful to Centre National d'Etudes Spatiales (CNES) and to ARIANE GROUP for using the test rig BALAFRE and for their agreement to present this experimental work. This work was partially funded by the French Government program "Investissements d'Avenir" (EQUIPEX GAP, reference ANR-11-EQPX-0018).

REFERENCES

[1] S. Charles, O. Bonneau, and J. Frêne. Determination of the discharge coefficient of a thin-walled orifice used in hydrostatic bearings. *ASME J. Tribol.*, 127(3):679–684, 2005.

[2] B. Jery, A. J. Acosta, C. E. Brennen, and T. K. Caughey. Hydrodynamic impeller stiffness, damping, and inertia in the rotordynamics of centrifugal flow pumps. In *In: Rotordynamic instability problems in high-performance turbomachinery: proceedings of a workshop held at Texas A M University, May 28-30*, 1984.

[3] Y. Yoshida, Y. Tsujimoto, D. Yokoyama, H. Ohashi, and Kano F. Rotordynamic fluid force moments on an open-type centrifugal compressor impeller in precessing motion. *International Journal of Rotating Machinery*, 7(4):237–251, 2001.

[4] D. Valentini, G. Pace, A. Pasini, L. Torre, R. Hadavandi, and L. d'Agostino. Analyses of hydrodynamic radial forces on centrifugal pump impellers. *European Journal of Mechanics - B/Fluids*, 61:336–345, 2017.

[5] U. Bolleter, A. Wyss, I. Welte, and R. Sturchler. Measurement of hydrodynamic interaction matrices of boiler feed pump impellers. *ASME. J. Vib., Acoust.*, 109(2):144–151, 1987.

[6] M. Uchiumi, N. Nagao, Y. Yoshida, and M. Eguchi. Comparison of rotordynamic fluid forces between closed impeller and open impeller. In *Proceedings of ASME. Fluids Engineering Division Summer Meeting, Rio Grande, Puerto Rico, July 8–12*, 2013.

[7] P. Jolly, A. Hassini, M. Arghir, and O. Bonneau. Experimental and theoretical rotordynamic coefficients of smooth and round-hole pattern water fed annular seals. In *Proceedings of ASME Turbo Expo 2014: Turbine Technical Conference and Exposition, Düsseldorf, Germany, June 16–20*, 2014.

[8] M. A. Corbo and S. B. Malanoski. Pump rotordynamics made simple. In *Proceedings of the Fifteenth International Pump Users Symposium, Turbomachinery Laboratory Texas A M University, College Station, Texas*, pages 167–204, 1998.

[9] M.L. Adams. *Rotating machinery vibration from analysis to troubleshooting*. Marcel Dekker, New York, 2001.

[10] D.R. Adkins and C.E. Brennen. Analyses of hydrodynamic radial forces on centrifugal pump impellers. *ASME. J. Fluids Eng.*, 110(1):20–28, 1988.

[11] J. M. VANCE, B. MURPHY, and F. ZEIDAN. *Machinery vibration and rotordynamics.* Hoboken, N.J., Wiley, 2010.

[12] N. Nagao, M. Eguchi, M. Uchiumi, and Y. Yoshida. Rotordynamic forces acting on a centrifugal open impeller in whirling motion by using active magnetic bearing. *Progress in Propulsion Physics*, 4:445–456, 2013.

[5] According to Ariane Group, those results, are in terms of quality and quantity, in good agreement with their computed results.

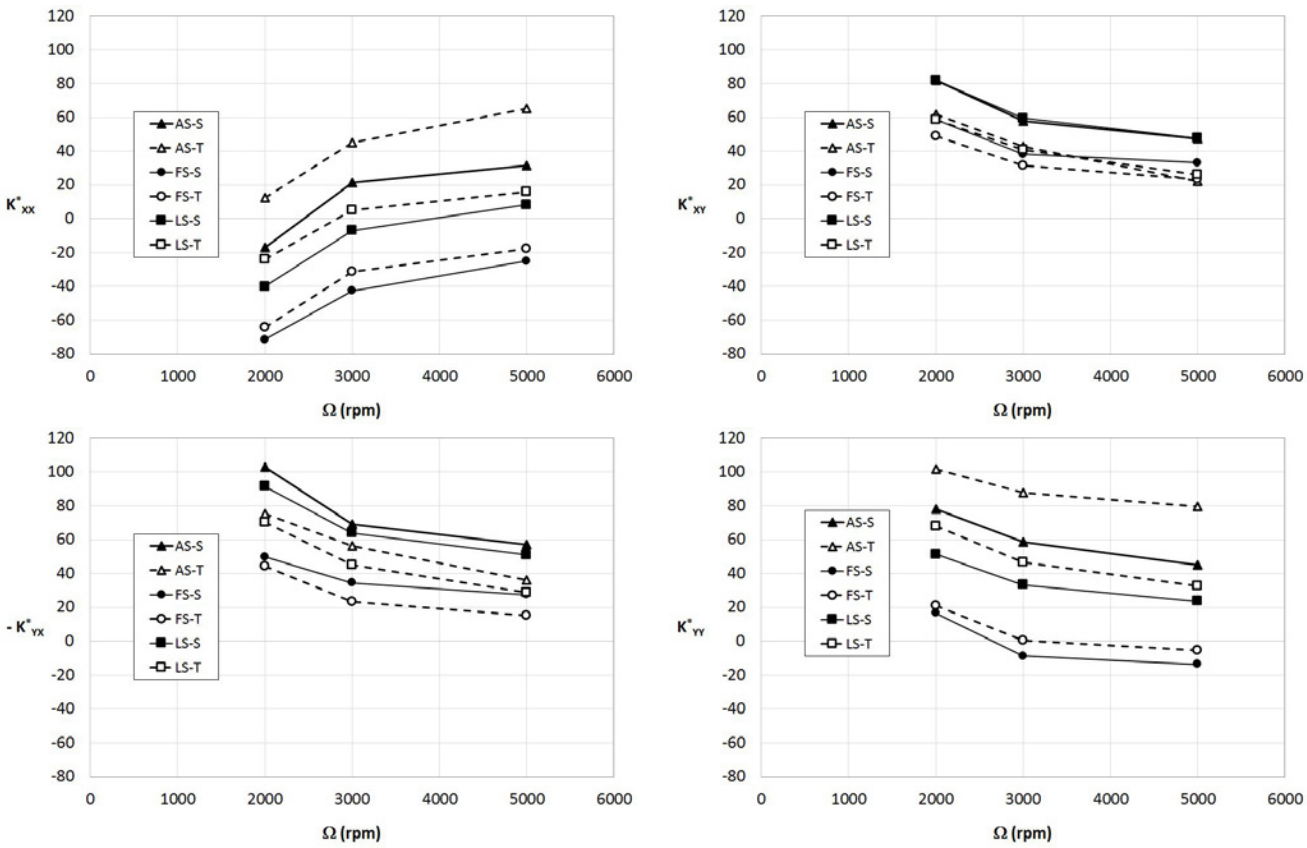

Figure 5. Dimensionless Measured Stiffness Coefficients K^*_{ij} according to the 6 tested configurations

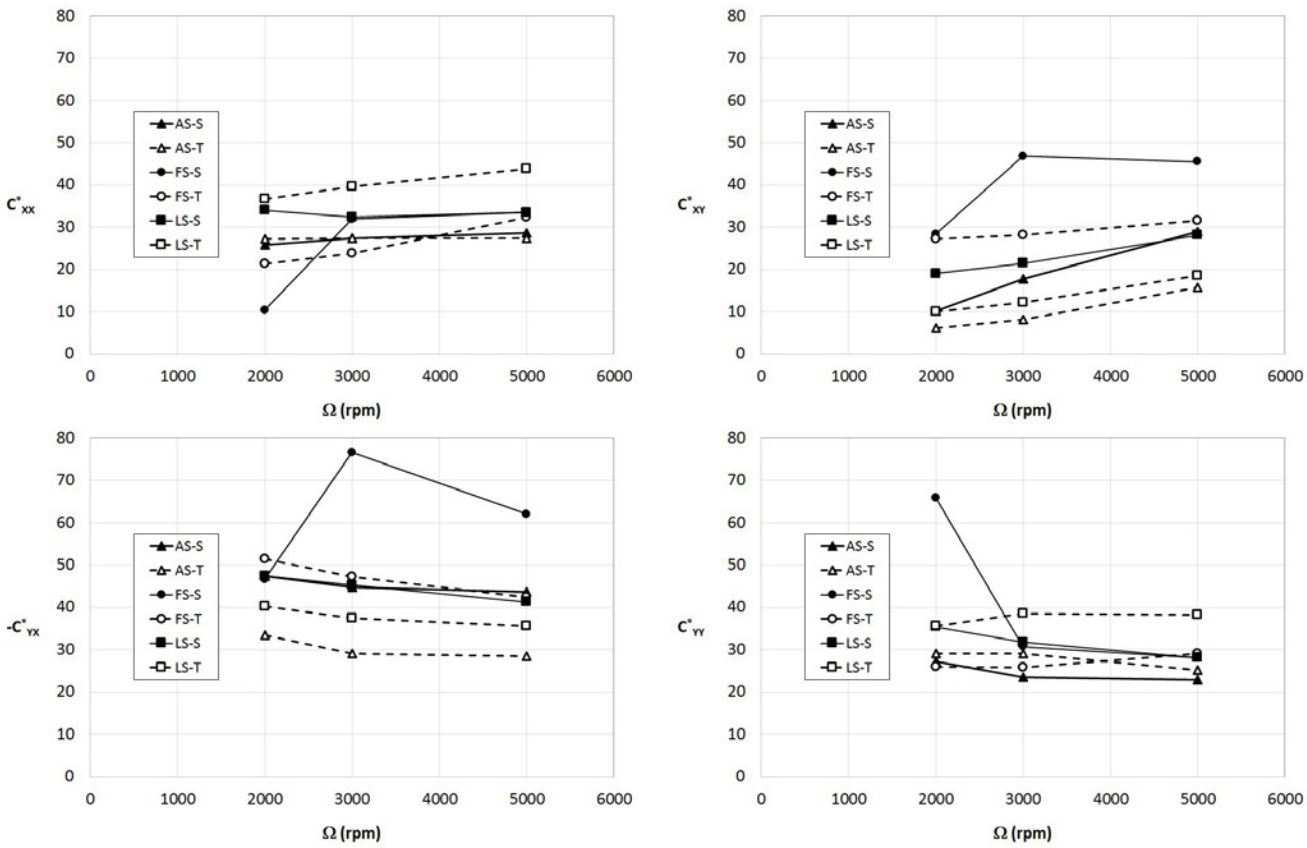

Figure 6. Dimensionless Measured Damping Coefficients C^*_{ij} according to the 6 tested configurations